

In Origin of Matter & Evolution of Galaxies 2003  
M. Terasawa et al., eds.  
World Scientific Publishing Co., 2005

## PROBING THE GALACTIC CHEMICAL EVOLUTION OF SI AND TI WITH PRESOLAR SiC GRAINS

SACHIKO AMARI<sup>†</sup>, ERNST ZINNER<sup>†</sup>

*Laboratory for Space Sciences and the Physics Department, Washington University,  
St. Louis, Missouri 63130, USA*

ROBERTO GALLINO\*

*Dipartimento di Fisica Generale dell'Universita' di Torino, 10125 Torino, Italy  
Centre for Stellar and Planetary Astrophysics, School of Mathematical Sciences,  
Monash University 3800 Victoria, Australia*

MARIA LUGARO\*

*Institute of Astronomy, University of Cambridge, Cambridge, CB3 0HA, UK*

OSCAR STRANIERO

*INAF-Osservatorio Astronomico di Teramo, I-64100 Teramo, Italy*

INMA DOMÍNGUEZ

*Departamento de Física Teórica y del Cosmos, Universidad de Granada, E-18071  
Granada, Spain*

Presolar SiC grains of the types mainstream, Y, and Z are believed to have formed in thermally pulsing asymptotic giant branch stars with a range of metallicity: mainstream grains in stars of close-to-solar metallicity, Y grains in stars of around half-solar metallicity, and Z grains in stars of around one-third solar metallicity. From their Si and Ti isotopic ratios, it is possible to obtain information on both neutron capture processes that take place in the He intershell and initial compositions of the parent stars of the grains. Since Z grains formed in stars with the lowest metallicity, their study will likely provide insight into the Galactic chemical evolution of these elements as well as nuclear processes in low-metallicity stars. A preliminary comparison of data on Z grains with models of AGB stars confirms that Z grains formed in low-metallicity stars ( $Z \leq 0.006$ ). The  $^{12}\text{C}/^{13}\text{C}$  ratios of the Z grains indicate that in these stars cool bottom processing operates during the third dredge-up.

### 1. Introduction

Our solar system formed from a collapsing molecular cloud 4.6 billion years ago. Until the late sixties, it was believed that solid material in the molecular

---

<sup>†</sup> This work is supported by NASA grant NAG5-11545.

\* This work is supported by Italian FIRB Project "Astrophysical Origin of the Heavy Elements Beyond Fe".

cloud completely evaporated during this event and thus the solar system was isotopically homogenized. This notion had been widely accepted since isotopic ratios of bulk meteorites, the only extra-terrestrial object available at that time, were identical to those of terrestrial material.

The first indication of the preservation of extra-solar material came from isotopically anomalous noble gases in primitive meteorites. When Black and Pepin [1] heated six carbonaceous chondrites in incremental temperature steps and analyzed isotopic ratios of Ne released in each step, in the temperature fractions between 900 and 1000°C they observed low ratios ( $^{20}\text{Ne}/^{22}\text{Ne}$  down to 3.4,  $^{20}\text{Ne}/^{22}\text{Ne}_{\text{air}}=9.8$ ) that had previously not been seen in meteorites. Later, this Ne-rich component was named Ne-E [2]. It has been proposed that the low  $^{20}\text{Ne}/^{22}\text{Ne}$  ratio is due to  $^{22}\text{Na}$  that decays to  $^{22}\text{Ne}$  with half life of 2.6 years [3]. As this component is observed in only a few temperature steps, the fraction of the anomalous noble gas relative to the total  $^{22}\text{Ne}$  in meteorites is very small ( $\sim 7 \times 10^{-4}$  in the Orgueil meteorite). Isotopically anomalous components have been also observed for Kr and Xe. The Kr and Xe components that are enriched in even-number isotopes are called Kr-S and Xe-S, respectively, because this pattern is the signature of the *s*-process [4]. Xenon that is enriched in both light and heavy isotopes has been named Xe-HL; it most likely originated from supernovae [5].

The minerals that contained the anomalous noble gases are what we now call presolar grains. Presolar grains formed in stellar outflows or stellar ejecta, and were incorporated into meteorites where they retained their distinct isotopic ratios. At the time these anomalous noble gas components were discovered, the carrier minerals were not known although subsequent studies indicated that they seemed to be carbonaceous. Thus, Edward Anders, Roy S. Lewis and their colleagues at the University of Chicago, the group that finally succeeded in isolating the minerals, temporarily gave the carriers alphabetical names such as C $\square$  and C $\square$  during their search [6]. In 1987, diamonds, which carry Xe-HL were finally isolated from a meteorite [7], followed by SiC [8, 9] and graphite [10].

Presolar grains that do not contain anomalous noble gases have been identified by secondary ion mass spectrometry (SIMS) single-grain isotopic analysis. Oxide grains were located in acid resistant residues from meteorites because of their anomalous O isotopic ratios [11-13]. Recently, advances in SIMS instrumentation [14] have made it possible to identify presolar silicate grains in interplanetary dust particles [15] and the Acfer094 meteorite [16] by their anomalous O isotopic ratios. Other mineral types of presolar grains identified up to date include refractory carbides [17, 18] and silicon nitride [19].

## 2. Silicon carbide grains of an AGB star origin

### 2.1. Carbon, N and Si isotopic ratios of SiC grains

Of the types of presolar grains, SiC has been most extensively studied. The reason is that the extraction procedure of SiC is straightforward compared with that of graphite [20]. Furthermore, SiC grains occur in various kinds of meteorites [21] with relatively high abundances (6ppm in the Murchison meteorite). Most data on single SiC grains have been obtained by ion probe isotopic analysis. In Figure 1, which shows C and N isotopic ratios of SiC grains, the data points cluster in specific regions. This fact led to the classification of SiC grains into populations according to their C, N and Si isotopic ratios (Figs. 1 and 2).

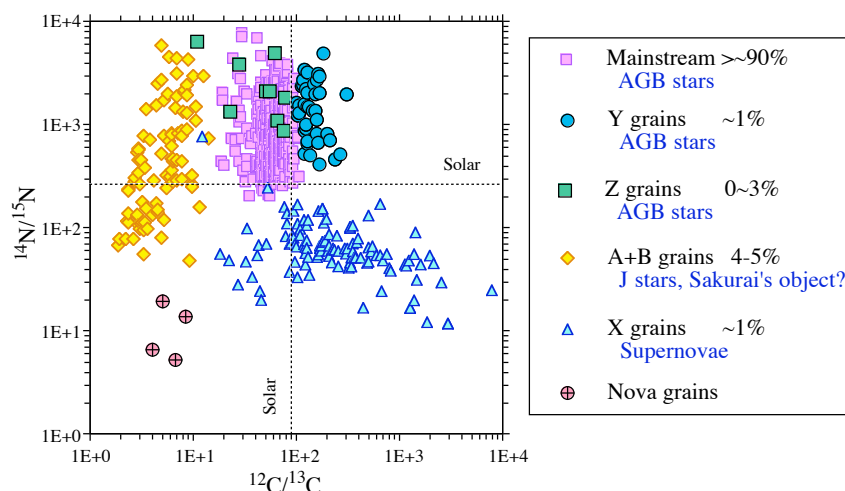


Figure 1. Carbon and N isotopic ratios of SiC grains. The grains have been classified into several populations based on their C, N and Si isotopic ratios. Abundances and proposed stellar sources of the populations are shown in the legend. Error bars are smaller than the symbols. Data are from [19, 22-28].

Mainstream grains, making up more than 90% of presolar SiC, have lower  $^{12}\text{C}/^{13}\text{C}$  and higher  $^{14}\text{N}/^{15}\text{N}$  ratios than the sun [22]. We note that grains of the minor populations, which comprise the rest, are overrepresented in Figs. 1 and 2 because they were preferentially studied after having been identified by a technique called ion imaging (their abundances are shown in the legend of Fig. 1). A+B grains are defined as having  $^{12}\text{C}/^{13}\text{C}$  ratios lower than 10 with a range of  $^{14}\text{N}/^{15}\text{N}$  ratios. Since it is difficult to explain the spread of the  $^{14}\text{N}/^{15}\text{N}$  ratios by one type of stellar source, at least two types of stellar sources seem to exist

for this population [25]. X grains are characterized by  $^{28}\text{Si}$  excesses up to 5 times solar in addition to higher-than-solar  $^{12}\text{C}/^{13}\text{C}$ , and lower-than-solar  $^{14}\text{N}/^{15}\text{N}$  ratios. They most likely formed in supernovae [29]. Only a handful of putative nova grains with low  $^{12}\text{C}/^{13}\text{C}$  and  $^{14}\text{N}/^{15}\text{N}$  ratios have been identified [30].

Grains of type Y and Z exhibit higher-than-solar  $^{14}\text{N}/^{15}\text{N}$  ratios, similar to mainstream grains. Y grains are defined as having  $^{12}\text{C}/^{13}\text{C} > 100$  [23], while Z grains show  $^{12}\text{C}/^{13}\text{C}$  ratios similar to those of mainstream grains [24]. Silicon isotopic ratios in mainstream, Y and Z grains show a systematic trend. First, average  $^{29}\text{Si}/^{28}\text{Si}$  ratios systematically decrease from mainstream to Y to Z grains ( $\epsilon^{29}\text{Si}/^{28}\text{Si} = 55 \pm 46$ ,  $18 \pm 36$ , and  $-76 \pm 57\%$ , where  $\epsilon^{i}\text{Si}/^{28}\text{Si}(\%) \equiv [(^{i}\text{Si}/^{28}\text{Si})_{\text{grain}} / (^{i}\text{Si}/^{28}\text{Si})_{\text{solar}} - 1] \times 1000$ ). Second, the spread of  $\epsilon^{30}\text{Si}/^{28}\text{Si}$  values systematically becomes larger: average  $\epsilon^{30}\text{Si}/^{28}\text{Si}$  values with standard deviations are  $44 \pm 36$ ,  $67 \pm 43$ , and  $91 \pm 170\%$  for mainstream, Y and Z grains, respectively. Grains of the three populations are believed to have formed in asymptotic giant branch (AGB) stars of a range of metallicity [31]: mainstream grains in AGB stars of close-to-solar metallicity [32], Y grains of around half solar metallicity [23], and Z grains of around one-third of solar metallicity [24].

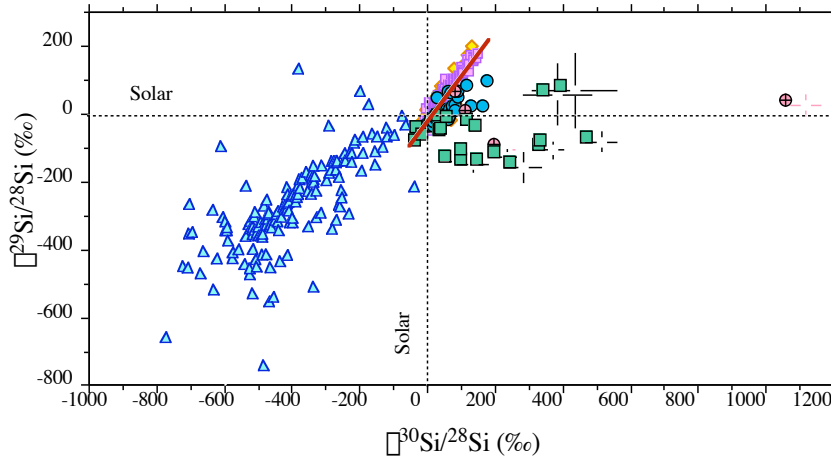


Figure 2. Silicon isotopic ratios of SiC grains expressed as  $\epsilon$  values, which are deviations from the solar ratios in parts per thousand. Data are from [19, 22-28]. Symbols are the same as in Fig. 1. The correlation line for the mainstream grain data is shown.

## 2.2. AGB star origin of mainstream, Y and Z grains

The strongest proof of an AGB star origin of the mainstream grains came from isotopic measurements of heavy elements on bulk samples (=aggregates of grains) and later on single grains. Since  $>90\%$  of the SiC grains are mainstream grains, bulk analyses can be regarded as representative of mainstream grains. s-

Process isotopic ratios inferred from the grain analyses agree quite well with average ratios predicted for low-mass ( $1-3M_{\odot}$ ) AGB stars with solar metallicity [32], as shown in Fig. 3 in the case of Xe [33]. A good agreement is also observed for Kr, Sr, Xe, Ba, Nd, and Sm (bulk analyses) [32] as well as Zr and Mo (single grain analyses) [34, 35].

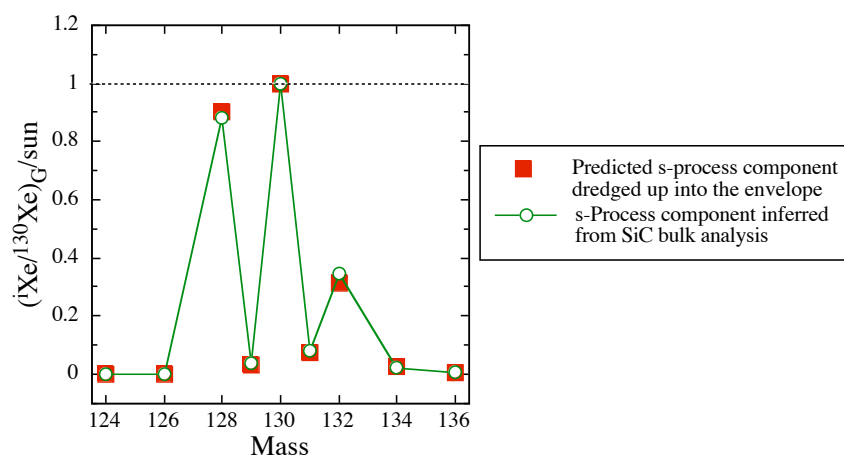


Figure 3. *s*-Process Xe inferred from noble gas analysis of aggregates of SiC grains (open circles) [36, 37] agrees with theoretical predictions of cumulative *s*-process Xe that is dredged up into the envelope during third dredge up episode (denoted as “G” in the ordinate) in low-mass AGB stars with solar metallicity [33].

An AGB star origin of Y and Z grains has been concluded from the similarity of isotopic ratios of light elements to those of mainstream grains and comparison with model calculations [23, 24].

Silicon isotopic ratios of the mainstream grains bear the signature of both, the original composition of the grains’ parent stars and neutron-capture that took place inside stars. However, the latter is not as pronounced as the *s*-process signature in the heavy elements. Silicon data of the mainstream grains plot along a line in a Si 3-isotope plot (Fig. 2). Expected isotopic shifts due to neutron capture (27‰ in  $^{30}\text{Si}/^{28}\text{Si}$  in  $2M_{\odot}$  stars of solar metallicity) are much smaller than the whole range observed in the grains (–50 to 100‰). Furthermore, the slope due to neutron capture process (0.11) is expected to be much smaller than the slope of the mainstream correlation line (1.31). Thus the linear trend has been interpreted as representing the initial compositions of parent stars of the mainstream grains, which in turn are determined by the Galactic chemical evolution.

### 2.3. Silicon and Ti

The fact that Si in mainstream grains reflects two factors, neutron-capture in stars and the Galactic chemical evolution, can be well understood if we consider grain formation in AGB stars. Condensation temperatures of SiC depend on the total pressure. For assumed pressures of  $10^{-5}$  to  $10^{-3}$  bars ( $10$ – $1000$  dyn/cm<sup>2</sup>) and C/O=1.05, SiC grains are expected to condense at  $\sim 1900$  to  $1500$  K [38]. Thus, they formed in the stellar outflow, far away from the photosphere (where the temperature is estimated to be  $2650$  K). For SiC to condense the gas has to be C-rich. Otherwise, all C combines with O to form CO, which is a very stable molecule, and C is not available for the formation of carbonaceous grains. Meanwhile, in the He-rich region located between the H shell and He shell (He intershell) convective instabilities are episodically triggered by the thermal instability occurring periodically in the He shell (thermal pulses). After the quenching of a pulse, material from the He intershell, enriched in  $^4\text{He}$ ,  $^{12}\text{C}$  and *s*-process elements, is mixed with material in the convective envelope (third dredge-up) when the convective envelope penetrates in the upper region of the He-intershell, which eventually makes the envelope C-rich [39]. The conditions of low temperature and C>O require that the SiC grains formed in the stellar outflow during and/or after third dredge-up. The composition of the envelope during that period is the result of mixing between two components, the initial composition of the star and that of the burnt material in the He shell and He intershell.

It is estimated that overproduction factors of  $^{28}\text{Si}$  and  $^{48}\text{Ti}$  that are processed in the He intershell and dredged up into the envelope (averages of  $1.5$  and  $3M_{\odot}$  stars of half solar metallicity), so-called the G-component, are  $1.09$  and  $0.77$ , respectively, while those of *s*-process only isotopes such as  $^{96}\text{Mo}$  and  $^{138}\text{Ba}$  are  $1000$ , which for the heavy elements results in a complete domination of the nucleosynthesis component in the mix.

It should be pointed out that, of the trace elements found in SiC, Ti is the third most abundant element after N and Al and this enables us to make Ti isotopic measurements with relatively small errors.

### 2.4. Z grains

Among the three SiC populations with an AGB star origin, Z grains are of a particular interest, since they formed in stars of the lowest metallicity [24]. The Z grains that were studied were analyzed for isotopic ratios of only one or two elements in addition to Si. This is because they are more abundant among small grains ( $<1\mu\text{m}$ ) and most studies on SiC have been performed for grains larger

than 1  $\mu\text{m}$ . Two grains were analyzed for Ti isotopic ratios (Fig. 4) [40] with a new type of ion probe, the NanoSIMS [14].

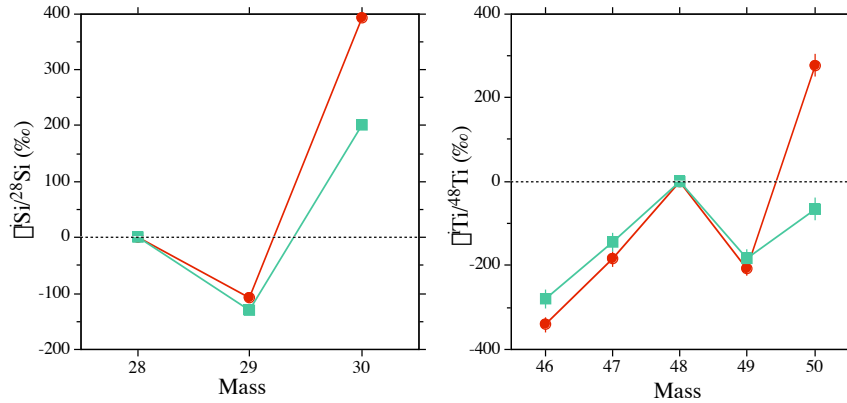


Figure 4. Silicon and Ti isotopic ratios of two Z grains. The grains show strikingly similar isotopic patterns except for  $^{30}\text{Si}/^{28}\text{Si}$  and  $^{50}\text{Ti}/^{48}\text{Ti}$  ratios. The dotted lines represent solar isotopic ratios.

The two Z grains have relatively high  $^{12}\text{C}/^{13}\text{C}$  ratios ( $93.5 \pm 0.6$  and  $81.1 \pm 0.5$ ) but exhibit the typical Si isotopic signature of Z grains with  $^{29}\text{Si}$  depletions and  $^{30}\text{Si}$  enhancements. Their Ti isotopic patterns are striking. Titanium-46,  $^{47}\text{Ti}$  and  $^{49}\text{Ti}$  are depleted relative to  $^{48}\text{Ti}$  to the same extent in the two grains, while their  $^{50}\text{Ti}/^{48}\text{Ti}$  ratios are quite different. One grain has a  $^{50}\text{Ti}$  excess ( $^{50}\text{Ti}/^{48}\text{Ti} = 276 \pm 26\%$ ), while the other one has a deficit ( $^{50}\text{Ti}/^{48}\text{Ti} = -66 \pm 25\%$ ). These  $^{50}\text{Ti}/^{48}\text{Ti}$  ratios are positively correlated with the  $^{30}\text{Si}/^{28}\text{Si}$  ratios of these two grains. During the third dredge-up, the  $^{30}\text{Si}/^{28}\text{Si}$  and  $^{50}\text{Ti}/^{48}\text{Ti}$  ratios in the envelope are expected to increase more than the other Si and Ti isotopic ratios, leading to relative  $^{30}\text{Si}$  and  $^{50}\text{Ti}$  excesses. The correlation thus reflects the result of nuclear processes in the He-intershell. After the addition of the material from the He-intershell that is enriched in neutron-rich Si and Ti isotopes, the isotopic ratios of the grains (except  $^{30}\text{Si}/^{28}\text{Si}$  ratios and a  $^{50}\text{Ti}/^{48}\text{Ti}$  ratio of one of the grains) are still lower than solar. This indicates that all original Si and Ti isotopic ratios in the parent stars of the two Z grains were lower than solar, suggesting stars of low metallicity.

### 3. Models of AGB stars

We have made a comparison between the Z grain data and predicted ratios in models of AGB stars. To model the nucleosynthesis in the He intershell, a post-processing code that computes neutron captures on nuclei from He to Bi [41] was used. The evolution of the nuclear abundances at the stellar surface is

subsequently calculated by mixing He intershell material by third dredge-up with a mass-losing envelope. Stellar structure features such as the envelope mass, the dredged-up mass, the temperature and density at the base of the convective pulse, as well as their trends in time and in mass during the convective thermal pulse, are needed as inputs in the post-processing code. The stellar structure parameters for a large number of models were obtained from the analytic formulas for AGB stars of masses  $\leq 3M_{\odot}$  provided by Straniero et al. [42]. These formulas were generated by interpolating the results of a set of stellar models which were previously evolved using the Frascati Raphson Newton Evolutionary Code (FRANEC) [43]. The model grid covers the following masses:  $M=1.5$  and  $3M_{\odot}$  and metallicities:  $Z=0.01$ ,  $0.006$  and  $0.003$ . Mass loss during the AGB phase is included by following the prescription of Reimers as expressed by the parameter  $\eta$  [44].

For the C/O ratio of solar metallicity, we used a revised value of  $0.50 \pm 0.07$  from newly acquired spectroscopic data of the solar photosphere [45, 46]. Alpha enhancement, the linear enrichment of  $\alpha$  elements with decreasing  $[\text{Fe}/\text{H}]$  down to  $-1$ , was taken into account for  $^{12}\text{C}$  as well as  $^{28}\text{Si}$  and  $^{48}\text{Ti}$  based on the observation by Reddy et al. [47]. The adopted  $^{16}\text{O}$  enhancement is based on the observation by Abia et al. [48]. The initial Si isotopic ratios are assumed to be  $-175\%$  for  $Z=0.003$ ,  $-115\%$  for  $Z=0.006$ , and  $-70\%$  for  $Z=0.01$ , and the initial Ti isotopic ratios to be  $-380\%$  for  $Z=0.003$ , and  $-260\%$  for  $Z=0.006$ .

### 3.1. Comparison between the grain data and the models

#### 3.1.1. Silicon

The Si isotopic ratios of the Z grains and several cases of the model calculations are shown in a Si 3-isotope plot (Fig. 5). The spread of Si isotopic ratios in the models depends on both mass that is dredged up into the envelope and the maximum temperature at the bottom of the convective He-flash zone. The former increases with increasing mass, decreasing metallicity, and decreasing Reimers mass loss parameter  $\eta$ , whereas the latter increases with decreasing metallicity. The  $Z=0.003$  and  $Z=0.006$  models cover the data points fairly well. Since the  $Z=0.01$  cases cover only a small range of the grain data, the Z grains more likely have formed in lower metallicity stars.

A point where the models do not agree with the data is the  $^{12}\text{C}/^{13}\text{C}$  ratios. Whereas C isotopic ratios of the Z grains are in the same range as those of mainstream grains, the models predict that at the end of third dredge up,  $^{12}\text{C}/^{13}\text{C}$  ratios in the envelope are high in low-metallicity stars (855 for  $3M_{\odot}$  stars of  $Z=0.006$ ). In order to explain the  $^{12}\text{C}/^{13}\text{C}$  ratios of the Z grains, Hoppe et al.



[24] invoked cool bottom processing (CBP) after the first dredge up and before the AGB phase [49-52], which is considered to take place in stars with mass of less than  $2.3M_{\odot}$ .

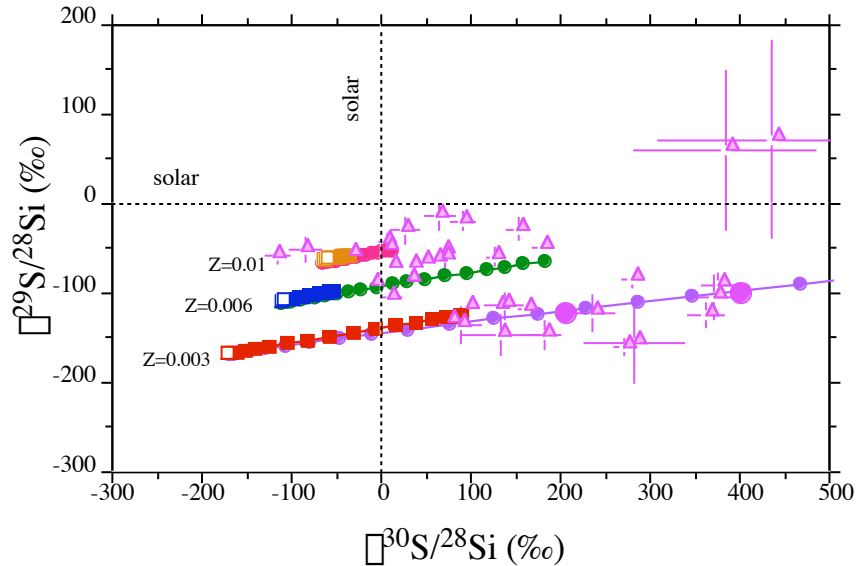


Figure 5. Triangles represent Z grain data obtained by [24, 53-55]. The two solid circles are the grains for which Ti isotopic ratios had been measured [40]. Squares indicate  $M=1.5M_{\odot}$  models, while circles  $M=3M_{\odot}$  models. Reimers mass loss parameter  $\eta$  is 0.3 for all cases. Open symbols indicate ratios when the envelope is O-rich and solid symbols when it is C-rich.

Nollett et al. [56] proposed that cool bottom processing (CBP) occurs also during the thermally pulsing phase of AGB stars. Hot bottom burning (HBB) that takes place in intermediate mass stars also produces low  $^{12}\text{C}/^{13}\text{C}$  ratios, but also high  $^{26}\text{Al}/^{27}\text{Al}$  ratios. The ratios of two Z grains ( $<2.9 \times 10^{-3}$ ,  $1.9 \pm 0.9 \times 10^{-3}$ ) [24] are lower than those predicted from models of HBB, indicating that CBP is a more likely process.

### 3.1.2. Titanium

With only two data points, it is not possible to see any trend. One piece of important information is that the initial  $^{47}\text{Ti}/^{48}\text{Ti}$  ratios are lower than the assumed values. Initial compositions may vary depending on a better fine-tuning for the choice of the  $\epsilon$ -enhancement. There is uncertainty of a factor of two on the Galactic chemical evolution inferred from spectroscopic observations. It should be also noted that Ti cross sections have uncertainties of about 10%

(□). New measurements of the Ti cross sections are expected to improve the precision of the model calculations.

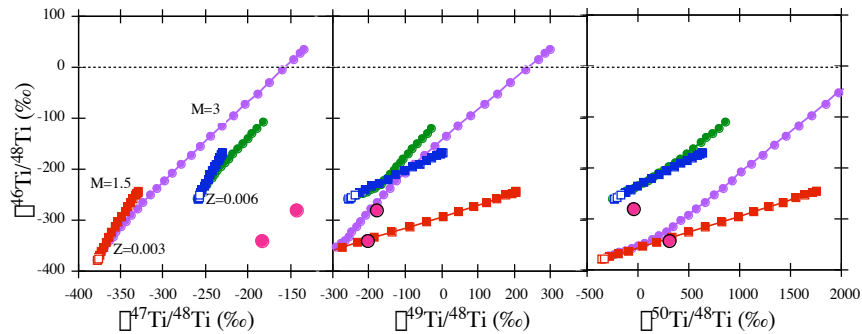


Figure 6. Titanium isotopic ratios of two Z grains and predicted ratios in the envelope. The symbols are the same as those in Fig. 5. The dotted lines indicate solar isotopic ratios.

#### 4. Future work

Obviously it is highly desirable to find more Z grains, analyze their Ti isotopic ratios and have a larger data set for Z grains. As for the other populations of grains of an AGB star origin, Ti isotopic ratios of Y grains have previously been analyzed [23]. However, the large errors of these measurements did not allow to detect a systematic difference between the Ti isotopic ratios of Y grains and mainstream grains [23]. Thus, it would also be helpful to reanalyze Ti isotopic ratios of Y grains with the NanoSIMS.

#### References

1. D. C. Black and R. O. Pepin, *Earth Planet. Sci. Lett.*, **6**, 395 (1969).
2. D. C. Black, *Geochim. Cosmochim. Acta*, **36**, 377 (1972).
3. D. D. Clayton, *Nature*, **257**, 36 (1975).
4. B. Srinivasan and E. Anders, *Science*, **201**, 51 (1978).
5. R. S. Lewis, B. Srinivasan and E. Anders, *Science*, **190**, 1251 (1975).
6. E. Anders In *Meteorites and the Early Solar System*, (J. F. Kerridge and M. S. Matthews) 927 University of Arizona Press, (1988).
7. R. S. Lewis, M. Tang, J. F. Wacker, E. Anders and E. Steel, *Nature*, **326**, 160 (1987).
8. T. Bernatowicz, G. Fraundorf, M. Tang, E. Anders, B. Wopenka, E. Zinner and P. Fraundorf, *Nature*, **330**, 728 (1987).
9. M. Tang and E. Anders, *Geochim. Cosmochim. Acta*, **52**, 1235 (1988).
10. S. Amari, E. Anders, A. Virag and E. Zinner, *Nature*, **345**, 238 (1990).
11. I. D. Hutcheon, G. R. Huss, A. J. Fahey and G. J. Wasserburg, *Astrophys. J.*, **425**, L97 (1994).

12. G. R. Huss, A. J. Fahey, R. Gallino and G. J. Wasserburg, *Astrophys. J.*, **430**, L81 (1994).
13. L. R. Nittler, C. M. O'D Alexander, X. Gao, R. M. Walker and E. Zinner, *Astrophys. J.*, **483**, 475 (1997).
14. F. J. Stadermann, R. M. Walker and E. Zinner, *Lunar Planet. Sci.*, **XXX**, Abstract #1407 (1999).
15. S. Messenger, L. P. Keller, F. J. Stadermann, R. M. Walker and E. Zinner, *Science*, **300**, 105 (2003).
16. A. N. Nguyen and E. Zinner, *Science*, in revision (2004).
17. T. J. Bernatowicz, S. Amari, E. K. Zinner and R. S. Lewis, *Astrophys. J.*, **373**, L73 (1991).
18. T. J. Bernatowicz, R. Cowsik, P. C. Gibbons, K. Lodders, B. Fegley, Jr., S. Amari and R. S. Lewis, *Astrophys. J.*, **472**, 760 (1996).
19. L. R. Nittler et al., *Astrophys. J.*, **453**, L25 (1995).
20. S. Amari, R. S. Lewis and E. Anders, *Geochim. Cosmochim. Acta*, **58**, 459 (1994).
21. G. R. Huss and R. S. Lewis, *Geochim. Cosmochim. Acta*, **59**, 115 (1995).
22. P. Hoppe, S. Amari, E. Zinner, T. Ireland and R. S. Lewis, *Astrophys. J.*, **430**, 870 (1994).
23. S. Amari, L. R. Nittler, E. Zinner, R. Gallino, M. Lugaro and R. S. Lewis, *Astrophys. J.*, **546**, 248 (2001).
24. P. Hoppe et al., *Astrophys. J.*, **487**, L101 (1997).
25. S. Amari, L. R. Nittler, E. Zinner, K. Lodders and R. S. Lewis, *Astrophys. J.*, **559**, 463 (2001).
26. S. Amari, P. Hoppe, E. Zinner and R. S. Lewis, *Astrophys. J.*, **394**, L43 (1992).
27. P. Hoppe, R. Strebel, P. Eberhardt, S. Amari and R. S. Lewis, *Meteorit. Planet. Sci.*, **35**, 1157 (2000).
28. S. Amari, X. Gao, L. Nittler, E. Zinner, J. José, M. Hernanz and R. Lewis, *Astrophys. J.*, **551**, 1065 (2001).
29. S. Amari and E. Zinner In *Astrophysical Implications of the Laboratory Study of Presolar Materials*, (T. J. Bernatowicz and E. Zinner) 287 AIP, New York (1997).
30. S. Amari, X. Gao, L. Nittler, E. Zinner, J. José, M. Hernanz and R. S. Lewis, *Astrophys. J.*, **551**, 1065 (2001).
31. E. Zinner, S. Amari, R. Gallino and M. Lugaro, *Nuclear Physics A*, **A688**, 102 (2001).
32. R. Gallino, M. Busso and M. Lugaro In *Astrophysical Implications of the Laboratory Study of Presolar Materials*, (T. J. Bernatowicz and E. Zinner) 115 AIP, New York (1997).
33. M. Pignatari, R. Gallino, R. Reifarth, F. Käppeler, S. Amari, A. M. Davis and R. S. Lewis, *Meteorit. Planet. Sci.*, **38**, A152 (2003).
34. G. K. Nicolussi, A. M. Davis, M. J. Pellin, R. S. Lewis, R. N. Clayton and S. Amari, *Science*, **277**, 1281 (1997).
35. G. K. Nicolussi, M. J. Pellin, R. S. Lewis, A. M. Davis, S. Amari and R. N. Clayton, *Geochim. Cosmochim. Acta*, **62**, 1093 (1998).
36. R. S. Lewis, S. Amari and E. Anders, *Nature*, **348**, 293 (1990).

37. R. S. Lewis, S. Amari and E. Anders, *Geochim. Cosmochim. Acta*, **58**, 471 (1994).
38. K. Lodders and B. Fegley Jr., *Meteoritics*, **30**, 661 (1995).
39. M. Busso, R. Gallino and G. J. Wasserburg, *Ann. Rev. Astron. Astrophys.*, **37**, 239 (1999).
40. S. Amari, E. Zinner, R. Gallino and C. S. Lewis, *Meteorit. Planet. Sci.*, **38**, A66 (2003).
41. R. Gallino et al., *Astrophys. J.*, **497**, 388 (1998).
42. O. Straniero, I. Domínguez, S. Cristallo and R. Gallino, *Publ. Astron. Soc. Australia*, **20**, 389 (2003).
43. O. Straniero, A. Chieffi, M. Limongi, M. Busso, R. Gallino and C. Arlandini, *Astrophys. J.*, **478**, 332 (1997).
44. D. Reimers In *Problems in stellar atmospheres and envelopes*, 229 Springer-verlag, New York (1975).
45. C. Allende Prieto, D. L. Lambert and M. Asplund, *Astrophys. J.*, **556**, L63 (2001).
46. C. Allende Prieto, D. L. Lambert and M. Asplund, *Astrophys. J.*, **573**, L137 (2002).
47. B. E. Reddy, J. Tomkin, D. L. Lambert and C. A. Prieto, *Mon. Not. R. Astron. Soc.*, **340**, 304 (2003).
48. C. Abia, M. Busso, R. Gallino, I. Domínguez, O. Straniero and J. Isern, *Astrophys. J.*, **559**, 1117 (2001).
49. D. S. P. Dearborn, P. P. Eggleton and D. N. Schramm, *Astrophys. J.*, **203**, 455 (1976).
50. A. V. Sweigart, L. Greggio and A. Renzini, *Astrophys. J. Suppl.*, **69**, 911 (1989).
51. C. Charbonnel, *Astron. Astrophys.*, **282**, 811 (1994).
52. A. I. Boothroyd and I.-J. Sackmann, *Astrophys. J.*, **510**, 232 (1999).
53. C. M. O'D Alexander, *Geochim. Cosmochim. Acta*, **57**, 2869 (1993).
54. X. Gao and L. R. Nittler, *Lunar Planet. Sci.*, **XXVIII**, 393 (1997).
55. E. Zinner, S. Amari, R. Guinness and C. Jennings, *Meteorit. Planet. Sci.*, **38**, A60 (2003).
56. K. M. Nollett, M. Busso and G. J. Wasserburg, *Astrophys. J.*, **582**, 1036 (2003).